Proc. IAHS, 382, 683–687, 2020
https://doi.org/10.5194/piahs-382-683-2020

Remotely triggered subsidence acceleration in Mexico City induced by the September 2017 M_w 7.1 Puebla and the M_w 8.2 Tehuantepec September 2017 earthquakes

Dario Solano-Rojas[1], **Enrique Cabral-Cano**[2], **Enrique Fernández-Torres**[2], **Emre Havazli**[3,a], **Shimon Wdowinski**[4], **and Luis Salazar-Tlaczani**[2]

[1]Facultad de Ingeniería, Universidad Nacional Autónoma de México, México City, CDMX, México
[2]Instituto de Geofísica, Universidad Nacional Autónoma de México, México City, CDMX, México
[3]Rosenstiel School of Marine and Atmospheric Science, University of Miami, Miami, Florida, USA
[4]Department of Earth and Environment, Florida International University, Miami, FL, USA
[a]now at: Institute of Technology, Jet Propulsion Laboratory California, Pasadena, CA, USA

Correspondence: Enrique Cabral-Cano (ecabral@igeofisica.unam.mx)

Published: 22 April 2020

Abstract. Mexico City, a large megacity with over 21 million inhabitants, is exposed to several hazards, including land subsidence, earthquakes, and flooding. Hazard assessments for each hazard type is typically treated separately and usually do not include considerations for any relations among the hazards. Our data makes it plausible for an earthquake triggering case that temporarily accelerated the subsidence rate in the metropolitan area as a result of the M_w 8.2 Tehuantepec and the M_w 7.1 Puebla, September 2017 earthquakes that affected Mexico City. Furthermore, the triggering effect induced rapid slip along previously developed shallow faults associated with subsidence. These results indicate that any future scenario of land subsidence should consider a potential triggering effect by large earthquakes. Similarly, earthquake hazard assessments should also consider potential impact on shallow faulting and fracturing associated with land subsidence.

1 Land subsidence in Mexico City

Mexico City is one of the fastest-subsiding metropolises in the world, where subsidence rates exceed 360 mm yr^{-1} (Fig. 1). The subsidence occurs mainly as the response to aggressive groundwater extraction over the past century, causing progressive damage to the city's buildings and critical infrastructure. The subsidence process has been documented for almost a century (Gayol, 1925; Carrillo, 1948; Figueroa-Vega, 1984; Ortega et al., 1993). Subsidence rates vary spatially, mainly due to highly heterogeneous shallow stratigraphic sequence beneath the city (Santoyo-Villa et al., 2005; Auvinet et al., 2017), which responds differentially to groundwater extraction. Highest subsidence rates occur above thick layers of lacustrine sediments (Cabral-Cano et al., 2008; Solano-Rojas et al., 2015), whereas non-subsiding areas correspond to volcanic rocks. Subsidence occurs differentially, particularly between stable volcanic rocks and highly subsiding sediments, producing significant topographic elevation changes and causing shallow faulting and fracturing along well-defined areas of the city (Fig. 2).

Mexico City subsidence has been studied in the past with conventional topographic methods (e.g., Auvinet et al., 2017). However, in the past decade subsidence has monitored by advanced satellite geodetic techniques, mainly satellite Interferometric Synthetic Aperture Radar (InSAR) and GPS (e.g. Cabral et al., 2008; López-Quiroz et al., 2009; Osmanoğlu et al., 2011; Du et al., 2019). These studies have routinely detected the highest subsidence rates in the eastern sector of the city within two areas that correspond to the former Texcoco and Chalco-Xochimilco lakes (Fig. 1). Moreover, most of the previous studies focused on the city-wide subsidence signal, which is important for understanding the city's aquifer mechanics in response to groundwater extraction. Both GPS and InSAR measurements indicated limited

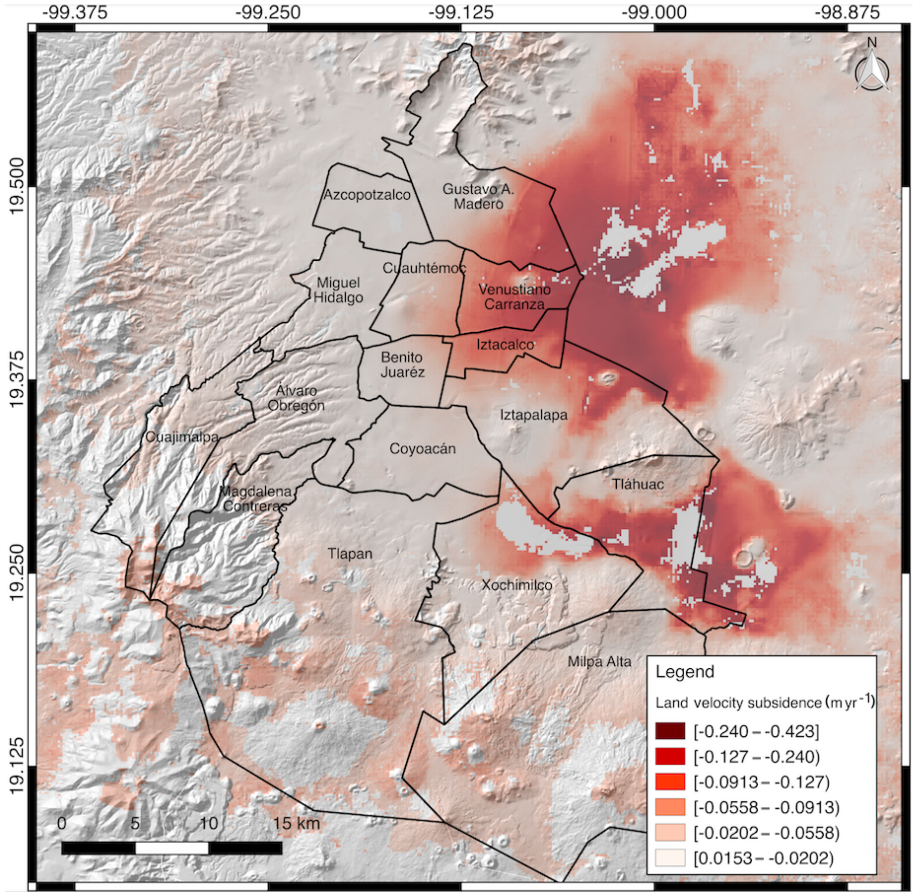

Figure 1. Subsidence velocity map for Mexico City and its municipalities (black lines) derived from the interferometric analysis of Sentinel-1 SAR data between November 2014 and November 2017. Black lines show Mexico City's municipalities. The shaded topographic base layer is taken from Continuo de Elevaciones Mexicano 3.0 © Instituto Nacional de Estadística Geografía e Informática (INEGI).

temporal changes in the subsidence rate throughout the past two decades with limited seasonal variability.

2 September 2017 earthquakes

Mexico City recently experienced two large earthquakes that took place only 11 d apart: the M_w 8.2 8 September 2017 with its epicenter offshore Chiapas, and the M_w 7.1 19 September 2017 with its epicenter in Puebla (Singh et al., 2018). The epicenter of the M_w 8.2 earthquake was located over 700 km away from Mexico City causing only minor impact to the city. However, the epicenter of the M_w 7.1 earthquake occurred only $\sim$ 100 km away from the city, which resulted in severe damaged in the city. Mexico City is very susceptible to seismic-induced damage, because part of the city is built over a sedimentary basin with clay rich lacustrine sediments up to 400 m thick (Santoyo-Villa et al., 2006; Auvinet et al., 2017). This sedimentary unit amplifies seismic energy causing site effects and making buildings and infrastructures more vulnerable, depending on their locations within the city.

Local seismic acceleration and site effects have been previously studied as part of the city building code developed after the M_w 8.2 1985 earthquake. However, not much attention has been paid to the shallow faulting associated with land subsidence that has developed on the transitional zones between the lacustrine deposits and the volcanic structures outcropping and its role as a potential risk during large earthquakes. This situation creates a strong horizontal gradient of subsidence where faulting and fracturing of the surface is common and is and addition element when considering the vulnerability for civil structural damage.

3 Remotely triggered subsidence acceleration

We use satellite-acquired SAR data from the Sentinel-1 satellites provided by the European Space Agency (ESA) through the Alaska Satellite Facility SAR Data Center repository. The InSAR process using ISCE software includes multilooking, topography removal, flattening, filtering, unwrapping, georeferencing and re-wrapping steps to obtain a longer-term baseline for the regional subsidence velocity (Fig. 1).

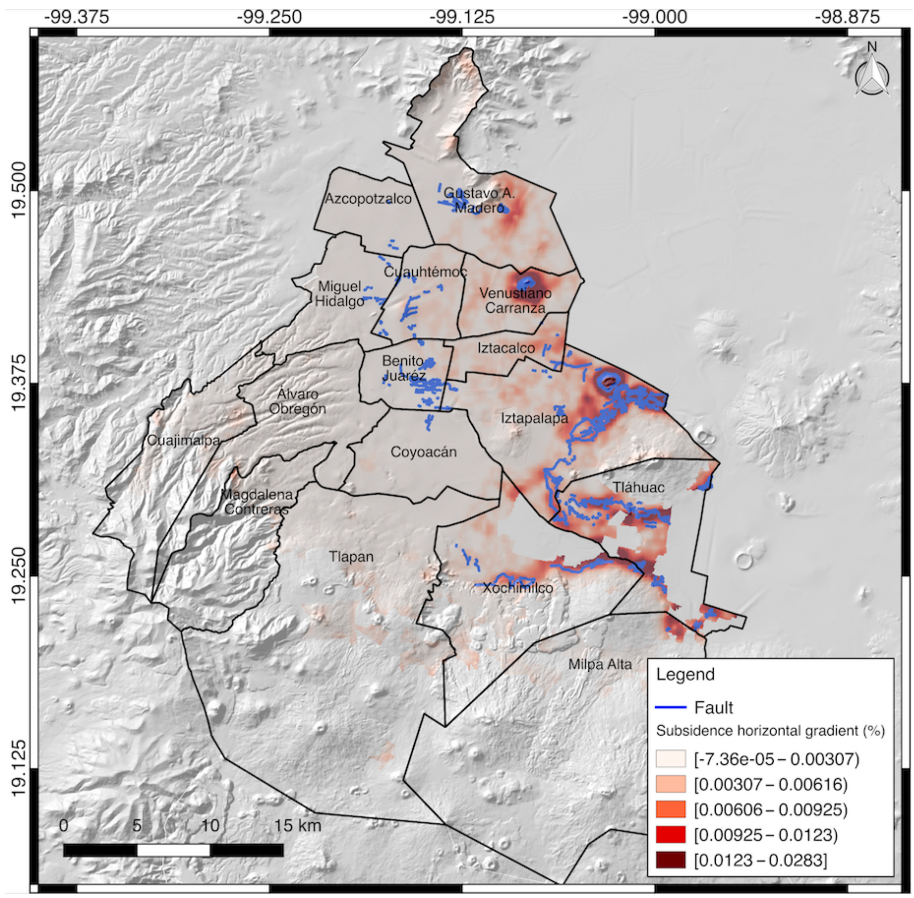

Figure 2. Horizontal subsidence gradient map for Mexico City derived from the Sentinel-1 velocity map (Fig. 1). Black lines show Mexico City's municipalities. Blue lines show the field mapped subsidence associated faults after CENAPRED (2017). The shaded topographic base layer is taken from Continuo de Elevaciones Mexicano 3.0 © Instituto Nacional de Estadística Geografía e Informática (INEGI).

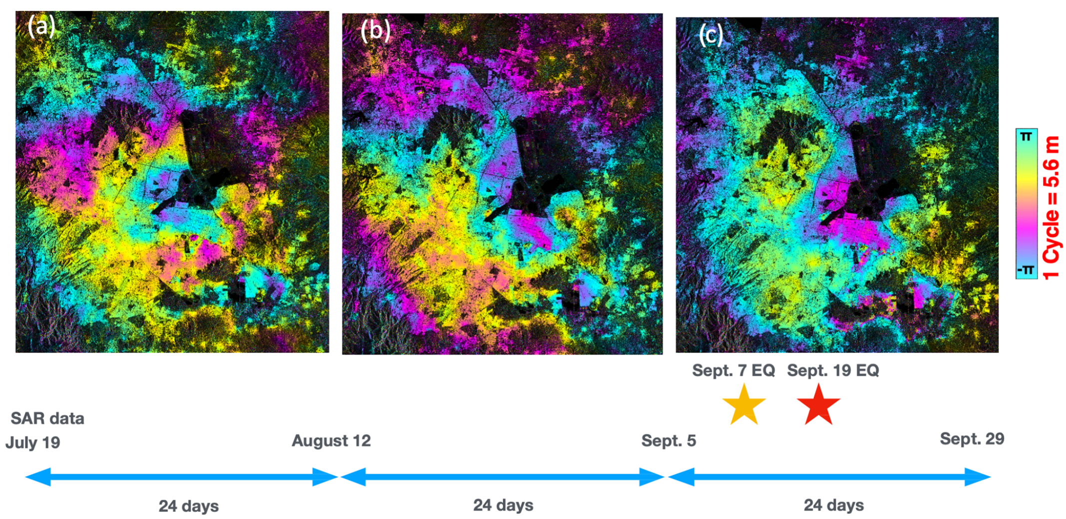

Figure 3. Sentinel-1 based wrapped differential interferograms for the Mexico City Metropolitan Area covering **(a)** 19 July–12 August 2017, **(b)** 12 August–5 September 2017, and **(c)** 5–29 September 2017. Color lookup table for all interferograms depicts 1 cycle = 6.6 cm.

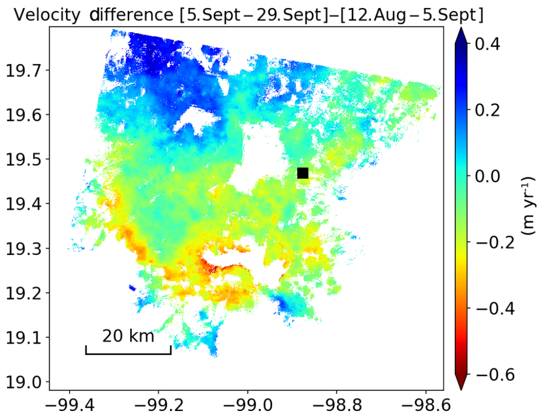

Figure 4. Subsidence velocity difference obtained by subtracting the 24 d subsidence vertical velocity field calculated from Fig. 3b prior to the M_w 8.2 Tehuantepec and the M_w 7.1 Puebla, September 2017 earthquakes vertical velocity field calculated from Fig. 3c.

We examined the effects of both earthquakes on the up to 360 mm yr^{-1} subsidence process in Mexico City using Sentinel-1 derived subsidence. As a baseline for pre-seismic deformation, we generated two 24 d SAR interferograms of data acquired between 19 July–12 August (Fig. 3a) and 12 August–5 September (Fig. 3b). These interferograms, covering the Mexico City Metropolitan area, show roughly 0.5–1 π phase change (light blue to purple), which is equivalent to 0.7–1.4 cm surface change in the highly subsiding regions within the city (Fig. 1). As the observed subsidence occurred over a period of 24 d, the two interferograms reflect subsidence rate of roughly 100–200 mm yr^{-1}. We also processed a third differential interferogram of data acquired on 5 and 29 September, which encompasses the integrated deformation for both the M_w 8.2 and M_w 7.1 earthquakes (Fig. 3c). This interferogram shows that the previously mentioned areas underwent an increase subsidence with much larger spatial coverage in comparison to the previous interferograms (Fig. 3a and b) which are 24 and 48 d older. The change in subsidence velocities (up to $\sim$ 33 mm total vertical displacement, equivalent to $\sim$ 38 % rate increase over a 24 d time window) and areal extent integrated during both seismic events (Fig. 4) indicates that most of the seismically triggered subsidence centered on these rapidly subsiding areas.

It is indeed possible that the energy released during these earthquakes is responsible for a distinctive deformation velocity pattern that is not shared by other sectors of the city where the underlying lacustrine sediment package is either thinner or absent.

A closer analysis of this circumstance shows that a large portion of the reported subsidence associated damage correlates with the presence of preexistent, subsidence-related faults (CENAPRED, 2017). Moreover, we find evidence of phase discontinuities in the 5–29 September interferogram, which also correspond to these areas around the lower slopes of the Sierra de Santa Catarina.

We conclude that the seismic energy from both earthquakes induced a fast soil consolidation and triggered the coseismic faulting of the preexistent subsidence related faults. This circumstance not previously observed 32 years ago during the M_w 8.1 19 September 1985 earthquake creates a new variable that needs to be addressed in future updates to the building codes and urban zoning considerations in Mexico City.

4 Conclusions

Our data makes it plausible that the seismic energy released by the M_w 8.2 8 September 2017, and the M_w 7.1 19 September 2017 earthquakes induced fast soil consolidation within a short time span, and triggered slip on the preexisting subsidence associated faults. This effect has not been previously documented but may be triggered again during another strong earthquake. Future hazard assessments for Mexico City should consider this triggering mechanism for the assessment and the inclusion shallow faulting for future urban building code and land use.

Data availability. Sentinel-1a and b SAR data used on this work was provided by the European Space Agency (ESA) through the Alaska Satellite Facility SAR Data Center (ASF SDC) at https://www.asf.alaska.edu/ (last access: 14 April 2020, Alaska Satellite Facility SAR Data Center, 2020).

Author contributions. DSR provided formal analysis and methodology, ECC provided conceptualization of the project, investigation, resources and writing of original draft and supervision, EFT provided methodology, investigation and validation, EH provided interferometric analysis during his doctoral studies in University of Miami, SW provided investigation, supervision and review and editing of draft, LST provided investigation and validation.

Competing interests. The authors declare that they have no conflict of interest.

Special issue statement. This article is part of the special issue "TISOLS: the Tenth International Symposium On Land Subsidence – living with subsidence". It is a result of the Tenth International Symposium on Land Subsidence, Delft, the Netherlands, 17–21 May 2021.

Acknowledgements. We thank Yunjun Zhang, Yoangel Torres, Talib Oliver and Leonardo Reyes for their help. Enrique Fernández-Torres acknowledges support from CONACyT and Dario Solano-

Rojas acknowledges support from CONACyT and Fulbright-García Robles. SAR data was kindly provided by the European Space Agency (ESA). Part of the InSAR processing was done on UNAM-DGTIC's Miztli supercomputing facility with processing time granted by LANCAD and CONACyT.

Financial support. This research has been supported by the Universidad Nacional Autónoma de México, Dirección General de Asuntos del Personal Académico, DGAPA-PAPIIT projects IV100215 and IN104818-3 and Consejo Nacional de Ciencia y Tecnología (CONACyT) projects 256012 and 005955 to Enrique Cabral-Cano and NASA project NNX12AQ08G to Shimon Wdowinski.

References

Alaska Satellite Facility SAR Data Center: Sentinel-1 Interferometric Wide swath Track 143, Frame 3203, descending mode, acquired between 19/07/2017 and 29/09/2017, available at: https://www.asf.alaska.edu, last access: 14 April 2020.

Auvinet, G., Méndez, E., and Juárez, M.: El Subsuelo de la Ciudad de Mexico, Instituto de Ingenierìa, UNAM, Vol. III, 2017.

Cabral-Cano, E., Dixon, T. H., Miralles-Wilhelm, F., Sánchez-Zamora, O., Díaz-Molina, O., and Carande, R. E.: Space geodetic imaging of rapid ground subsidence in Mexico City, B. Geol. Soc. Am., 120, 1556–1566, 2008.

Carrillo, N.: Influence of artesian wells on the sinking of México City, in: Proceedings of the Second International Conference on Soils Mechanics, Rotterdam, Holland, International Society for Soil Mechanics and Geotechnical Engineering, vol. VII, 1948.

CENAPRED: Análisis de la Vulnerabilidad Física a la Subsidencia y agrietamiento en la Ciudad de México, Centro de Geociencias, Universidad Nacional Autónoma de México, México, 23 pp., 2017.

Du, Z., Ge, L., Ng, A. H.-M., Zhu, Q., Zhang, Q., Kuang, J., and Dong, Y.: Long-term subsidence in Mexico City from 2004 to 2018 revealed by five synthetic aperture radar sensors, Land Degrad. Dev., 1–17, 2019.

Figueroa-Vega, F.: Case history no. 9.8, Mexico, in: Guidebook to Studies of Land Subsidence due to Ground-Water Withdrawal, edited by: Poland, J. F., United Nations Educational Scientific and Cultural Organization, Paris, France, 217–232, 1984.

Gayol, R.: Estudio de las perturbaciones que en el fondo de la Ciudad de México ha producido el drenaje de las aguas del subsuelo, por las obras del desague y rectificación de los errores a que ha dado lugar una incorrecta interpretación de los efectos producidos, Rev. Mex. Ing. Arquit., 3, 96–132, 1925.

López-Quiroz, P., Doin, M. P., Tupin, F., Briole, P., and Nicolas, J. M.: Time-series analysis of Mexico City subsidence constrained by radar interferometry, J. Appl. Geophys., 69, 1–15, 2009.

Ortega, A., Cherry, J. A., and Rudolph, D. L.: Largescale aquitard consolidation near Mexico City, Ground Water, 31, 708–718, 1993.

Osmanoğlu, B., Dixon, T. H., Wdowinski, S., Cabral-Cano, E., and Jiang, Y.: Mexico City subsidence observed with persistent scatterer InSAR, Int. J. Appl. Earth Obs. Geoinf., 13, 1–12, 2011.

Santoyo-Villa, E., Ovando-Shelley, E., Mooser, F., and Leon-Plata, E.: Síntesis Geotécnica de la Cuenca del Valle de México, Publicaciones TGC, Mexico City, México, 1st edn., vol. 1, 2005.

Singh, S. K., Reinoso, E., Arroyo, D., Ordaz, M., Cruz-Atienza, V., Pérez-Campos, X., Iglesias, A., and Hjörleifsdóttir, V.: Deadly Intraslab Mexico Earthquake of 19 September 2017 (M_w 7.1): Ground Motion and Damage Pattern in Mexico City, Seismol. Res. Lett., 89, 2193–2203, 2018.

Solano-Rojas, D., Cabral-Cano, E., Hernández-Espriú, A., Wdowinski, S., DeMets, C., Salazar-Tlaczani, L., Falorni, G., and Bohane, A.: La Relación de Subsidencia del Terreno GPS-InSAR y el abatimiento del nivel estático en pozos de la zona Metropolitana de la Ciudad de México, B. Soc. Geol. Mex., 67, 273–283, 2015.